Acta Crystallographica Section F
Structural Biology and Crystallization Communications
ISSN 1744-3091

Crystallization and preliminary X-ray analysis of the tumour necrosis factor α–tumour necrosis factor receptor type 2 complex

Yohei Mukai,[a,b] Teruya Nakamura,[c] Yasuo Yoshioka,[b,d] Shin-ichi Tsunoda,[b] Haruhiko Kamada,[b] Shinsaku Nakagawa,[a] Yuriko Yamagata[c] and Yasuo Tsutsumi[a,b]*

[a]Graduate School of Pharmaceutical Sciences, Osaka University, Japan, [b]Laboratory of Pharmaceutical Proteomics, National Institute of Biomedical Innovation (NiBio), Japan, [c]Graduate School of Pharmaceutical Sciences, Kumamoto University, Japan, and [d]The Center of Advanced Medical Engineering and Informatics, Osaka University, Japan

Correspondence e-mail: ytsutsumi@phs.osaka-u.ac.jp

Received 29 September 2008
Accepted 7 February 2009

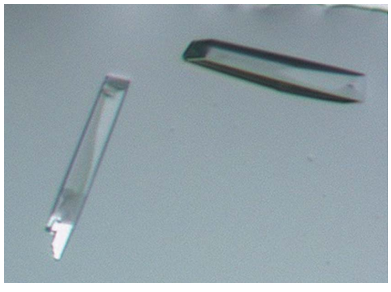

Tumour necrosis factor receptor type 2 (TNFR2, TNFRSF1B) is an essential receptor for various host-defence functions of tumour necrosis factor α (TNF). As part of studies to determine the structure of TNFR2, the formation, crystallization and preliminary X-ray diffraction analysis of the TNF–TNFR2 complex are described. The TNF–TNFR2 complex, which comprises one TNF trimer and three TNFR2 monomers, was confirmed and purified by size-exclusion chromatography. Crystals of the TNF–TNFR2 complex were obtained using polyethylene glycol 3350 as a precipitant. The crystal belonged to space group $P2_12_12_1$, with unit-cell parameters a = 74.5, b = 117.4, c = 246.8 Å. Assuming the presence of two TNF–TNFR2 complexes in the asymmetric unit, the Matthews coefficient V_M was 2.49 Å^3 Da^{-1} and the solvent content of the crystal was 50.7%. The crystal diffracted to 2.95 Å resolution.

1. Introduction

Tumour necrosis factor α (TNF) is a major inflammatory cytokine that plays a central role in host defence and inflammation (Aggarwal, 2003). Overexpression of TNF is closely associated with inflammatory diseases such as rheumatoid arthritis and inflammatory bowel disease (Feldmann & Maini, 2003). Therefore, anti-TNF antibodies and soluble TNF receptors (TNFR) that interfere with the activity of TNF have been used to treat various inflammatory diseases (Feldmann, 2002). However, anti-TNF therapy inhibits both types of TNFR (TNFR1 and TNFR2), often causing serious side effects.

Previous studies using animal models of diseases such as arthritis and hepatitis have demonstrated that TNFR1 plays a predominant role in the pathogenesis and exacerbation of inflammation (Mori *et al.*, 1996; Leist *et al.*, 1995). In contrast, TNFR2 is crucial for the proliferation, activation and antigen presentation of T cells, which are essential processes in the cell-mediated immune response against bacteria and viruses (Kafrouni *et al.*, 2003; Grell *et al.*, 1998). Therefore, blocking TNFR1-mediated signal transduction has emerged as a potential therapeutic strategy against inflammatory diseases with a low risk of side effects. Modelling the three-dimensional structure of the TNF–TNFR complex and understanding the differences between TNFR1 and TNFR2 will strongly contribute to the development of a TNFR1-selective therapeutic strategy.

To date, two crystal structures of TNFR1 have been reported: unliganded extracellular domains (PDB codes 1ncf and 1ext; Naismith *et al.*, 1995, 1996) and a lymphotoxin α (LT-α)–TNFR1 complex (PDB code 1tnr; Banner *et al.*, 1993). The structure of wild-type TNF has also been reported (PDB code 1tnf; Eck & Sprang, 1989). Several structures of TNF mutants, including the TNF mutant used in this experiment, have also been reported (PDB codes 1a8m, 2az5, 4tsv, 5tsw, 2e7a and 2zjc; Reed *et al.*, 1997; Cha *et al.*, 1998; Shibata *et al.*, 2008; Mukai *et al.*, 2009). However, the structure of TNFR2 has not yet been reported, although the structure of a viral protein with homology to TNFR2 has been solved (PDB code 2uwi; Graham *et al.*, 2007). This hinders the design of a structure-based drug for advanced anti-TNF therapy. Here, we describe the formation, crystallization and preliminary X-ray diffraction analysis of the

TNF–TNFR2 complex as part of our studies to determine the novel TNFR2 structure and aid in the development of TNFR1-selective therapies.

2. Methods

2.1. Preparation of TNF and TNFR2

The TNF molecule used in this experiment was a Lys-deficient TNF mutant [mutTNF Lys(−); K11M, K65S, K90P, K98R, K112N and K128P] created from wild-type TNF (wtTNF; NCBI accession No. X01394; Uniprot reference P01375) using a phage display system. This mutant retained full bioactivity and affinity for TNFR, as described previously (Yamamoto *et al.*, 2003). The wtTNF–TNFR2 complex formed efficiently, similar to that of mutTNF Lys(−) and TNFR2, but did not crystallize under the conditions described below.

MutTNF Lys(−) (residues 77–233 in Uniprot P01375; 157 amino acids, without tags) was expressed in *Escherichia coli* and refolded from inclusion bodies as described previously (Yamamoto *et al.*, 2003). Briefly, TNF was produced in *E. coli* BL21 (DE3) as inclusion bodies, which were washed in a buffer containing Triton X-100 and solubilized in 6 *M* guanidine–HCl, 0.1 *M* Tris–HCl pH 8.0 and 2 m*M* EDTA. Solubilized protein at 10 mg ml^{-1} was reduced with 65 m*M* dithioerythritol and refolded by a 100-fold dilution in a refolding buffer (100 m*M* Tris–HCl, 2 m*M* EDTA, 0.5 *M* arginine and 0.9 m*M* oxidized glutathione). After dialysis against 20 m*M* Tris–HCl pH 7.4 containing 100 m*M* urea, active trimeric proteins were purified by ion-exchange chromatography using Q-Sepharose FF (GE Healthcare Ltd). Size-exclusion chromatography was performed using a Superose 12 column (GE Healthcare) equilibrated with 20 m*M* Tris–HCl pH 7.4. The molecular mass of the purified TNF trimer was 51 kDa. The complete sequence of this TNF molecule was as follows: VRSSSRTPSD**M**PVAHVVANPQAEGQLQWLNRRANALLANG-VELRDNQLVVPSEGLYLIYSQVLF**S**GQGCPSTHVLLTHTISRI-AVSYQT**P**VNLLSAI**R**SPCQRETPEGAEA**N**PWYEPIYLGGVFQ-LE**P**GDRLSAEINRPDYLDFAESGQVYFGIIAL (residues mutated from wtTNF are shown in bold).

The extracellular domain of TNFR2 was used in this experiment (soluble TNFR2; NCBI accession No. M32315; Uniprot reference P20333). Purified soluble TNFR2 (residues 33–205 in Uniprot P20333; 173 amino acids, without tags) expressed in *E. coli* was purchased from PeproTech Inc. The molecular mass was 19 kDa as a monomer. The complete sequence of this TNFR2 molecule was as follows: APEPGSTCRLREYYDQTAQMCCSKCSPGQHAKVFC-TKTSDTVCDSCEDSTYTQLWNWVPECLSCGSRCSSDQVETQ-ACTREQNRICTCRPGWYCALSKQEGCRLCAPLRKCRPGFG-VARPGTETSDVVCKPCAPGTFSNTTSSTDICRPHQICNVVAIP-GNASMDAVCTSTSP. Lyophilized TNFR2 was dissolved in 20 m*M* Tris–HCl pH 7.4 and used directly for complex formation.

2.2. Purification of the TNF–TNFR2 complex

It is known that one TNF trimer binds three TNFR2 monomers and forms the TNF–TNFR2 complex. For crystallization of the complex, we attempted to purify the full 110 kDa TNF–TNFR2 complex (one 51 kDa TNF trimer and three 19 kDa soluble TNFR2 monomers). The complex was formed by mixing TNF and TNFR2 for 30 min at room temperature. Complex solutions with various molar ratios of TNF and TNFR2 were prepared and the molecular masses were assessed by analytical gel-filtration chromatography using a tandem Superdex 75 10/300 GL/Superdex 200 10/300 GL column (GE Healthcare) in 20 m*M* Tris–HCl pH 7.4 (Fig. 1). The use of two gel-filtration columns with different exclusion limits was useful for separating the complex from uncomplexed TNF and TNFR2. In this analysis, low-molecular-weight and high-molecular-weight gel-filtration calibration kits (GE Healthcare) were used as protein standards. An increase in the mixing ratio of TNFR2 induced a shift

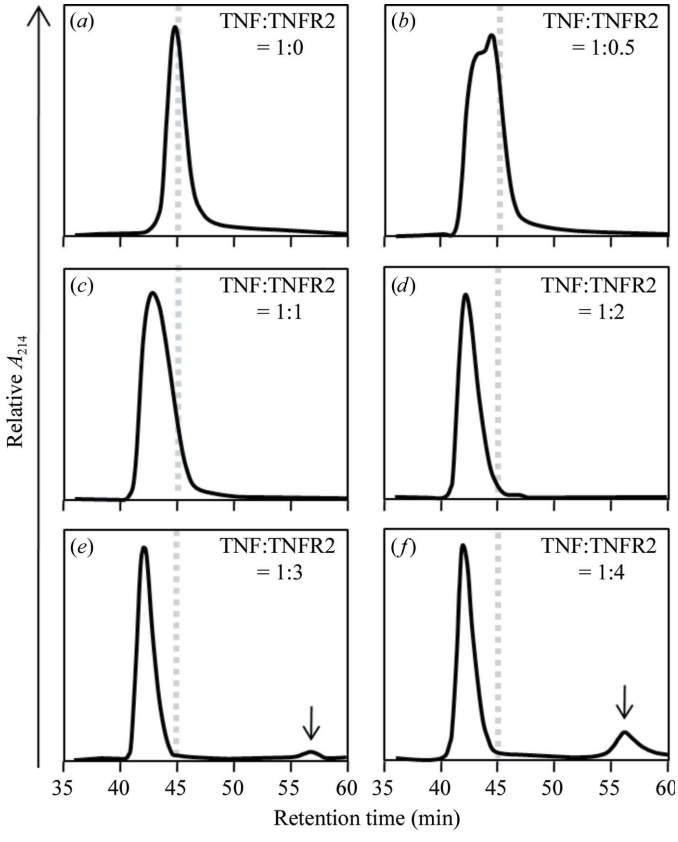

Figure 1
TNF–TNFR2 complex formation. Formation of the TNF–TNFR complex was assessed by analytical gel-filtration chromatography. The molar ratio of TNF trimer and TNFR2 was varied and the elution peak of the proteins was followed at 214 nm. The elution time of uncomplexed TNF occurs at 45 min (*a*). This is indicated by the broken grey line in (*a*)–(*f*). Excess unbound TNFR2 is indicated by arrows in (*e*) and (*f*).

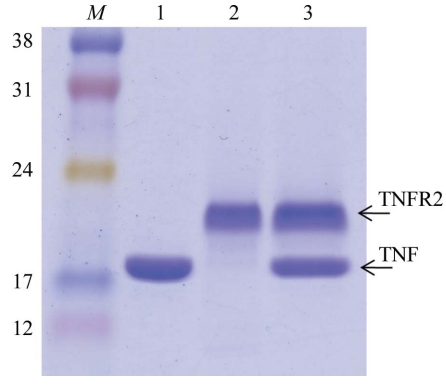

Figure 2
SDS–PAGE analysis of the TNF–TNFR2 complex. Formation of the TNF–TNFR2 complex was confirmed by SDS–PAGE. 15% polyacrylamide gel (ATTO Corp., Tokyo, Japan) was used to separate the bands containing TNF monomer (17 kDa) and TNFR2 monomer (19 kDa). *M*, Rainbow protein standard (labelled in kDa; GE Healthcare); lane 1, 2 µg TNF; lane 2, 2 µg TNFR2; lane 3, 4 µg purified TNF–TNFR2 complex.

in the retention peak of TNF to a higher molecular weight. At a TNF:TNFR2 ratio of 1:3 (Fig. 1*e*), a small peak at 57 min elution time corresponding to unbound 19 kDa TNFR2 was observed. This peak containing excess TNFR2 was also observed at a 1:4 ratio (Fig. 1*f*). This result indicated that the full 110 kDa TNF–TNFR2 complex was formed under these conditions. Therefore, final fractionation was performed between 41 and 44 min at a TNF:TNFR2 ratio of 1:4. The complex formation in the purified fraction was also confirmed by SDS–PAGE (Fig. 2). This full TNF–TNFR2 complex was concentrated to 10 mg ml^{-1} in 20 m*M* Tris–HCl pH 7.4 and used for crystallization as described below. The protein concentration was determined using Coomassie Protein Assay Reagent (Thermo Fisher Scientific Inc.).

2.3. Crystallization of the TNF–TNFR2 complex

The sparse-matrix screening kit Crystal Screen HT and the systematic salt and PEG screening kit Index HT (Hampton Research, Aliso Viejo, California, USA) were used for initial crystallization trials using the sitting-drop vapour-diffusion method. Drops consisting of 0.5 µl protein solution (10 mg ml^{-1}) and 0.5 µl reservoir solution were equilibrated against 100 µl reservoir solution in a Crystal*EX* 96-well flat-bottom plate (Corning Incorporated, Corning, New York, USA). Two temperatures, 293 and 277 K, were tested. Microcrystals were obtained using reservoir solution containing 20%(*w*/*v*) PEG 3350 and 0.2 *M* sodium formate at 293 K. A grid screen around these conditions was evaluated using the hanging-drop vapour-diffusion method. In this step, a drop consisting of 1 µl protein solution and 1 µl reservoir solution was equilibrated against 250 µl reservoir solution in a 24-well VDX Plate (Hampton Research). The crystallization conditions were improved using an additive screening kit (Hampton Research) and round-edged plate-shaped crystals were obtained from a droplet consisting of 1 µl 5 mg ml^{-1} protein solution and 1 µl reservoir solution containing 8%(*w*/*v*) PEG 3350, 0.2 *M* sodium formate and 0.02 *M* cobalt(II) chloride as an additive reagent. Protein and additive concentrations were optimized and the best crystals were obtained using 7.5 µl 0.8 mg ml^{-1} protein solution and 7.5 µl reservoir solution containing 7.5%(*w*/*v*) PEG 3350, 0.2 *M* sodium formate and 0.06 *M* cobalt(II) chloride. The crystals used for data collection had typical dimensions of 0.2 × 0.1 × 0.03 mm (Fig. 3).

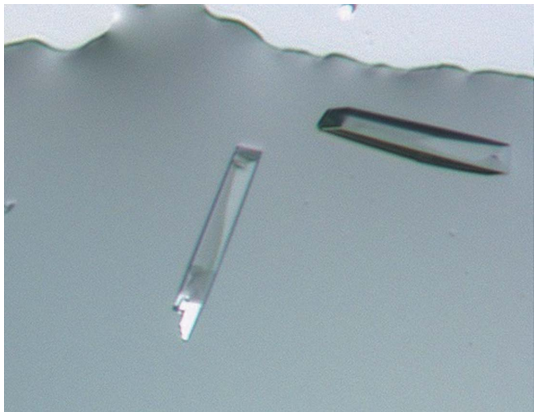

Figure 3
TNF–TNFR2 crystals. Two crystals of the TNF–TNFR2 complex with approximate dimensions of 0.2 × 0.1 × 0.03 mm are shown.

Table 1
Data-collection statistics for the TNF–TNFR2 complex.

Values in parentheses are for the highest resolution shell.

X-ray source	SPring-8 BL41XU
Wavelength (Å)	1.000
Space group	$P2_12_12_1$
Unit-cell parameters	a = 74.5, b = 117.4, c = 246.8
Resolution range (Å)	50–2.95 (3.06–2.95)
Observed reflections	744297
Unique reflections	45945 (4075)
Completeness (%)	98.9 (89.8)
$R_{\rm merge}$† (%)	0.183 (0.603)
$\langle I/\sigma(I)\rangle$	10.75 (1.51)

† $R_{\rm merge} = \sum_{hkl}\sum_i |I_i(hkl) - \langle I(hkl)\rangle| / \sum_{hkl}\sum_i I_i(hkl)$, where $I_i(hkl)$ is the ith intensity measurement of reflection hkl, including symmetry-related reflections, and $\langle I(hkl)\rangle$ is its average.

2.4. Preliminary X-ray analysis

X-ray diffraction experiments were performed on BL41XU of the SPring-8 Synchrotron Facility in Harima, Japan. An ADSC Quantum 315 X-ray CCD detector was installed on BL41XU and used to record the diffraction data. Crystals were soaked in a cryoprotectant solution composed of 7.5%(*w*/*v*) PEG 3350, 0.2 *M* sodium formate, 0.06 *M* cobalt(II) chloride and 30% glycerol. The crystals were then mounted in nylon loops (Hampton Research) and flash-cooled in a nitrogen stream at 95 K. Diffraction data were collected in 1.0° oscillation steps (180 images, 0–180°) and the crystal diffracted X-rays to 2.95 Å resolution. The data set was processed and scaled using the *HKL*-2000 program (Otwinowski & Minor, 1997). The crystals belonged to space group $P2_12_12_1$, with unit-cell parameters a = 74.5, b = 117.4, c = 246.8 Å. Data-collection statistics are shown in Table 1.

3. Results and discussion

The results of SDS–PAGE using the crystallization solution suggested that the crystal contained both TNF and TNFR2. Gel-filtration analysis showed that the TNF–TNFR2 complex with a molecular mass of 110 kDa contained both a TNF trimer (51 kDa) and three TNFR2 monomers (3 × 19 kDa). This suggests that the asymmetric unit of the crystals contained two molecules of the TNF–TNFR2 complex (two TNF trimers and six TNFR2 monomers). The calculated solvent content was 50.7% and the Matthews coefficient was 2.49 Å^3 Da^{-1} (Matthews, 1968).

Molecular replacement was performed with the *MOLREP* program (Vagin & Teplyakov, 1997) in *CCP*4*i* (Potterton *et al.*, 2003) using the TNF mutant structure described in our previous report (PDB code 2e7a; Shibata *et al.*, 2008) as a search model. Two significant solutions corresponding to TNF trimers were obtained (R = 0.469). The model from molecular replacement was subjected to rigid-body refinement, simulated annealing, energy minimization and *B*-factor refinement using *CNS* (Brünger *et al.*, 1998). The initial electron-density map calculated using only the phases of refined TNF trimer structures (R = 0.425 and $R_{\rm free}$ = 0.493) clearly showed almost the entire TNF trimer. The main chains and side chains of TNFR2 could also be detected around the TNF trimer. Manual model building of TNFR2 based on the TNFR1 structure using the *Coot* program (Emsley & Cowtan, 2004) in *CCP*4*i* is in progress.

This study was supported by Research for Promoting Technological Seeds (No. 11-067) from the Japan Science and Technology Agency (JST), Research Fund Project on Health Sciences focusing on Drug Innovation (No. KAA3701) from the Japan Health Sciences

Foundation, grants from the Ministry of Health, Labor and Welfare in Japan, a Grant-in-Aid for Young Scientists (B) (No. 20790134) and Grants-in-Aid for Scientific Research (Nos. 17016084, 17689008, 17790135, 18015055, 18659047, 20015052 and 20200017) from the Ministry of Education, Culture, Sports, Science and Technology of Japan (MEXT) and Research Fellowships for Young Scientists (No. 20-3919) from Japan Society for the Promotion of Science (JSPS). This study was also supported by Hayashibara Biochemical Laboratories Inc., Okayama, Japan.

References

Aggarwal, B. B. (2003). *Nature Rev. Immunol.* **3**, 745–756.
Banner, D. W., D'Arcy, A., Janes, W., Gentz, R., Schoenfeld, H. J., Broger, C., Loetscher, H. & Lesslauer, W. (1993). *Cell*, **73**, 431–445.
Brünger, A. T., Adams, P. D., Clore, G. M., DeLano, W. L., Gros, P., Grosse-Kunstleve, R. W., Jiang, J.-S., Kuszewski, J., Nilges, M., Pannu, N. S., Read, R. J., Rice, L. M., Simonson, T. & Warren, G. L. (1998). *Acta Cryst.* D**54**, 905–921.
Cha, S. S., Kim, J. S., Cho, H. S., Shin, N. K., Jeong, W., Shin, H. C., Kim, Y. J., Hahn, J. H. & Oh, B.-H. (1998). *J. Biol. Chem.* **273**, 21253–21260.
Eck, M. J. & Sprang, S. R. (1989). *J. Biol. Chem.* **264**, 17595–17605.
Emsley, P. & Cowtan, K. (2004). *Acta Cryst.* D**60**, 2126–2132.
Feldmann, M. (2002). *Nature Rev. Immunol.*, **2**, 364–371.
Feldmann, M. & Maini, R. N. (2003). *Nature Med.* **9**, 1245–1250.
Graham, S. C., Bahar, M. W., Abrescia, N. G., Smith, G. L., Stuart, D. I. & Grimes, J. M. (2007). *J. Mol. Biol.* **372**, 660–671.
Grell, M., Becke, F. M., Wajant, H., Mannel, D. N. & Scheurich, P. (1998). *Eur. J. Immunol.* **28**, 257–263.
Kafrouni, M. I., Brown, G. R. & Thiele, D. L. (2003). *J. Leukoc. Biol.* **74**, 564–571.
Leist, M., Gantner, F., Jilg, S. & Wendel, A. (1995). *J. Immunol.* **154**, 1307–1316.
Matthews, B. W. (1968). *J. Mol. Biol.* **33**, 491–497.
Mori, L., Iselin, S., De Libero, G. & Lesslauer, W. (1996). *J. Immunol.* **157**, 3178–3182.
Mukai, Y., Shibata, H., Nakamura, T., Yoshioka, Y., Abe, Y., Nomura, T., Taniai, M., Ohta, T., Ikemizu, S., Nakagawa, S., Tsunoda, S., Kamada, H., Yamagata, Y. & Tsutsumi, Y. (2009). *J. Mol. Biol.* **30**, 1121–1129.
Naismith, J. H., Devine, T. Q., Brandhuber, B. J. & Sprang, S. R. (1995). *J. Biol. Chem.* **270**, 13303–13307.
Naismith, J. H., Devine, T. Q., Kohno, T. & Sprang, S. R. (1996). *Structure*, **4**, 1251–1262.
Otwinowski, Z. & Minor, W. (1997). *Methods Enzymol.* **276**, 307–326.
Potterton, E., Briggs, P., Turkenburg, M. & Dodson, E. (2003). *Acta Cryst.* D**59**, 1131–1137.
Reed, C., Fu, Z. Q., Wu, J., Xue, Y. N., Harrison, R. W., Chen, M. J. & Weber, I. T. (1997). *Protein Eng.* **10**, 1101–1107.
Shibata, H. *et al.* (2008). *J. Biol. Chem.* **283**, 998–1007.
Vagin, A. & Teplyakov, A. (1997). *J. Appl. Cryst.* **30**, 1022–1025.
Yamamoto, Y., Tsutsumi, Y., Yoshioka, Y., Nishibata, T., Kobayashi, K., Okamoto, T., Mukai, Y., Shimizu, T., Nakagawa, S., Nagata, S. & Mayumi, T. (2003). *Nature Biotechnol.* **21**, 546–552.